DESIGN AND RESEARCH OF A CUTTING BLADE FOR CORN STALKS BASED ON A BIONIC PRINCIPLE
/
基于仿生原理的玉米秸秆切割刀片的设计与研究

Zhu ZHAO [1,2], Zhongnan WANG [2], Bintong ZHAO [1], Yuqiu SONG [1], Mingjin XIN *[1]
[1] College of Engineering, Shenyang Agricultural University, Shenyang / China;
[2] Liaoning Agricultural Technical College, Yingkou / China
Tel: +86-024-88487119; E-mail: xinmjsynd@163.com Corresponding author: Xin Mingjin
DOI: https://doi.org/10.35633/inmateh-68-70

Keywords: *Bionic blade, ant, mandible teeth, corn stalk, finite element analysis, cutting test*

ABSTRACT
The ant (Pheidole megacephala, Fabricius) has a unique and hard mandibular structure to cut branches and crush hard food. Inspired by this special geometric structure of the mandibular teeth, a stereoscopic microscope was used to view the image of the mandible of the ant. The Origin and AutoCAD software were used to obtain the outer profile of the mandibular teeth of the ant. The outer profile of the ant's mandibular teeth was fitted and expressed by five-order polynomial function. According to the analysis of the profile curve of the maxillary teeth, the fourth tooth is the most convex and the sharpest. The fourth tooth of the ant plays a key role in its feeding process, therefore, the structural parameters of the fourth maxillary tooth were selected as bionic elements for bionic blade design. To compare the cutting performance of the bionic and ordinary flat blades, the performance of bionic blade and the ordinary blade were conducted by using ANSYS software, the cutting force-deformation characteristics were tested using the Rapid TA practical texture analyser. The results of the element simulation showed that the mechanical properties of bionic blade were better than those of the ordinary blade. The results of the cutting experiments indicated that under the loading speed of 5 mm/s, the maximum cutting force of the bionic blade was 137.51 N, which is 12.17 % lower than that of the ordinary flat blade. The average cutting force of the bionic blade was 96.56 N, which is 11.58 % lower than that of the ordinary flat blade. The cutting energy consumption of the bionic blade was 9.68 J, which is 11.92 % lower than that of the ordinary flat blade. Under the loading speed of 10 mm/s, the maximum cutting force of the bionic blade was 143.88 N, which is 10.37 % lower than that of the ordinary flat blade. The average cutting force of the bionic blade was 101.03 N, which is 9.77 % lower than that of the ordinary flat blade. The cutting energy consumption of the bionic blade was 10.14 J, which is 9.95 % lower than that of the ordinary flat blade. The experimental results suggested that the bionic blade can effectively reduce the cutting force and energy consumption; thus, the bionic blade is more suitable for cutting stalks. These results will be helpful in the development of cutting elements for cutting and chopping of corn stover and other processing machinery.

摘要
蚂蚁(Pheidole megacephala, Fabricius)具有独特而坚硬的上颚结构，可以切割树枝和粉碎坚硬的食物。受到这种特殊的上颚齿几何结构的启发，我们用体式显微镜来观察蚂蚁的上颚齿结构，利用 Origin 软件和 AutoCAD 软件获得蚂蚁上颚齿的外轮廓曲线，用五阶多项式函数拟合和表示蚂蚁上颚齿的外轮廓曲线。根据上颚齿的轮廓曲线分析，得出蚂蚁上颚第 4 齿最为凸出和尖锐，在其取食过程中起着关键作用，因此，选择蚂蚁上颚第四齿的结构参数作为仿生刀片设计的仿生元素。为了比较仿生刀片和普通平刃刀片的切削性能，运用 ANSYS 软件对普通平刃刀和仿生刀片进行有限元静力学分析，采用 Rapid TA 实用型分析仪对其切削力-变形特性进行了测试。有限元仿真结果表明，仿生刀片的力学性能更优，切削实验结果表明，在 5mm/s 的加载速度下，仿生叶片的最大切削力为 137.31 N，比普通平刃刀片的最大切削力降低了 11.70%，仿生刀片的平均切削力为 96.56 N，比普通平板刀片的平均切削力低 11.58%，仿生刀片的切削能耗为 9.67 J，比普通平板刀片的切削能耗低 11.28%。在 10mm/s 的加载速度下，仿生叶片的最大切削力为 143.88N，比普通平刃刀片的最大切削力降低了 10.37%，仿生刀片的平均切削力为 101.03 N，比普通平板刀片的平均切削力低 9.77%，仿生刀片的切削能耗为 10.14J，比普通平板刀片的切削能耗低 9.95%。实验结果表明，该仿生刀片能有效降低切削力和能耗，仿生刀片更适合切割玉米茎秆。该研究将有助于玉米秸秆切割刀具和其他加工机械的开发。

[1] *Zhao Zhu, Ph.D. Stud. Eng.; Wang Zhongnan, Lab.Techo. MA. Eng.; Zhao Bintong, MA. Stud. Eng.; Song Yuqiu, Prof. Ph.D. Eng.; Xin Mingjin, Prof. Ph.D. Eng.*

INTRODUCTION

Cutting corn stalk is an important link in the working process of the corn harvester *(Jia et al., 2022)*. The cutting blade of the corn harvester determines the cutting quality of the corn stalk *(Zhao et al., 2022)*. At present, the cutting blade used in the corn harvesters mainly use flat blades, which are characterized by high cutting resistance, high energy consumption, and poor stubble quality (*Ma et al., 2020; Xu et al., 2021*). Therefore, there is a need to develop a cutting blade with low cutting resistance, low energy consumption, and high cutting quality.

Bionics is an interdisciplinary subject that bridges biology and engineering. By studying the structure, function, and operating principle of organisms, and applying these principles to engineering, it is possible to develop devices and machines with superior performance. It also provides researchers with new ideas and methods for improving the performance of cutting blades (*Chen et al., 2021; Zhang et al., 2022*). Studies on the cutting behaviour of various animals have produced several important theoretical results. The geometric structure and morphological outline of chewing mouthparts can help reduce cutting resistance during the predation and improve cutting quality. Massah et al. designed a corrugated blade based on the *Armadillidium vulgare* body surface geometrical shape. The experimental results showed that in wet soil, the corrugated blade resulted in the lowest drag force (*Massah et al., 2020*). Zhang et al. designed a bionic root cutter based on the contour curve model of the jaw of *Prosopocoilus astacoides*. The trial results showed that the effect of installing the bionic root cutter was better than that of an ordinary triangular root cutter (*Zhang et al., 2022*). Zhao et al. designed a bionic cutting blade that could reconstruct the multi-segment and serrated structure of locusts' mouthparts. The test results showed that the bionic cutting device could reduce the cutting torque and power consumption by 26.6-31.6 % and 21.9-26.1 %, respectively (*Zhao et al., 2020*). Tong et al. found that the contour curve of their incisors was close to the standard arc when studying the mouthparts of *Otidognathus davidis Fair* larvae. Based on this structure, a bionic cutting blade was designed. When cutting cabbage, the energy consumption of the bionic cutting blade was reduced by 12.8 % and the cutting performance was increased by 12.5 % (*Tong et al., 2017*). Tian et al. designed a hemp harvester blade based on the morphological characteristics of the incisors of the Longhorn beetle's mandible. They built a self-made double-acting blade cutting test bench to comparatively test the cutting of the bionic and ordinary blades. The average maximum cutting force and energy consumption of the bionic blade were reduced by 7.4 % and 8.0 %, respectively, and the bionic blade resulted in a significant reduction in resistance and consumption (*Tian et al., 2017*). Jia et al. designed a bionic saw blade inspired by the special geometric structure of incisors. The cutting force test showed that the bionic saw blade could lead to a noticeable reduction in cutting force and energy consumption (*Jia et al., 2013*).

The ant is one of the most widespread and abundant insect species on Earth (*Paul et al., 2003*). Ants have a unique and hard mandible structure that enables them to exert a large bite force to transport food, cut branches and leaves at high speed, and crush hard food (*Lei et al., 2016*). In this study, the ant's mandible was used as a bionic prototype, and its shape and structure were integrated into the design of the corn harvester's cutting blade. A stereoscopic microscope was used to access the ant's mandible image, and Origin and AutoCAD software were used to plot the ant's mandible characteristic curve. After analysing the maxillary teeth profile curve, the structural parameters of the fourth maxillary tooth of the ant were selected as the bionic elements for the bionic blade design. The bionic blade was made of metal and constructed using 3D printing technology. Corn stalk cutting tests were performed on a Rapid TA practical texture analyser to investigate the cutting capacity of the bionic blade against the ordinary flat blade in terms of cutting force and energy consumption.

MATERIALS AND METHODS

Observation and motion analysis of the ant mandible microstructure

The ant species selected in this experiment was *Camponotus japonicus*. Samples were collected from a farmer's corn planting base in Yingkou City, Liaoning Province, China. Scanning electron microscopy is the simplest and most effective method for observing microstructure and surface topography. A research-grade NSZ818 stereo microscope developed and manufactured by Ningbo Yongxin Optics Co., Ltd. was used in this experiment. The ant specimen was placed under the microscope for observation, the external structure and digital photograph of the ant sample is shown in Figure 1.

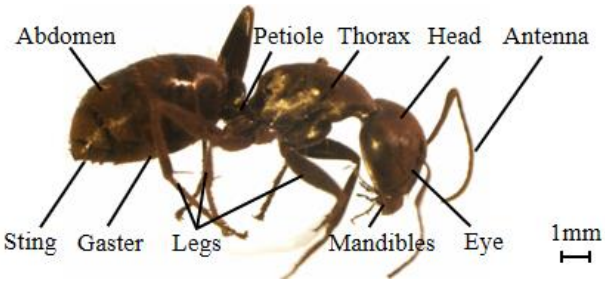

Fig. 1 - External structure of the ant sample

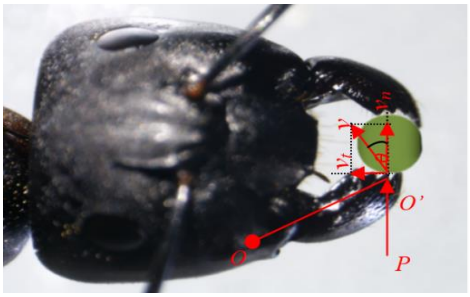

Fig. 2 - Ant occluding force vector diagram

Moreover, the focus knob was manually adjusted to focus on the ant's mandible. The lower jaw was observed moving around point *O*, and the bite force was detected at the end of the upper jaw. The direction of the absolute movement velocity of the upper jaw was neither vertical nor parallel to the cutting edge of the upper jaw. The movement of the ant's lower jaw results in sliding cutting. The absolute velocity was decomposed to obtain the normal and tangential velocities, as shown in Figure 2.

Based on Figure 2,

$$\tan\theta = \frac{v_t}{v_n} \tag{1}$$

Where: v_t is the tangential velocity, m/s; v_n is the normal velocity, m/s; θ is the angle between the absolute and normal velocities, that is, the slip cutting angle, °.

According to Gollum's constant theorem,

$$P^3 S = C \tag{2}$$

Where: P is the normal force required for test cutting depth, g; S is the tangential slip, mm; C is constant.

The Gollum constant theorem states that the greater the tangential slip, the lower the cutting force when the blade cuts into the same depth of material. In addition, the cutting angle is smaller during slip cutting, resulting in a lower cutting force.

Extraction of the ant maxillary tooth contour curve

The mandible was observed to have five teeth with a relatively uniform size and distribution. The anterior and lateral parts of the right mandible were viewed under a stereoscopic microscope, as shown in Figure 3.

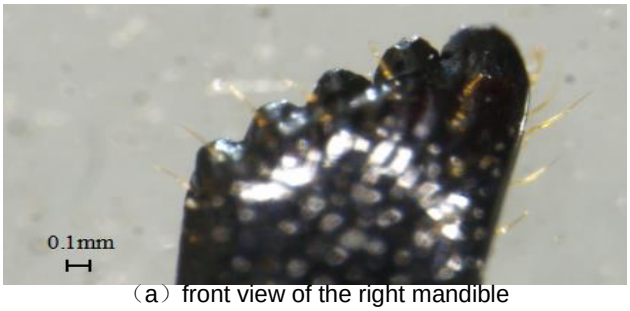

（a）front view of the right mandible

(b) side view of the right mandible

Fig. 3 - Digital photograph of the ant's mandible

To extract the ant maxillary tooth contour curve, Adobe Illustrator software was first used to convert the bitmap into a high-fidelity vector diagram, and all the geometric feature contour points of the teeth were extracted from the ant's mandible. To distinguish the target image from the image background, the vector image was binarized to plot a binarized image. AutoCAD software was used for further adjustment and plotting, which was used to extract the outline of the ant's maxillary tooth structure. Each black pixel in the image represents a two-dimensional variable, which is specified by coordinates. The extracted boundary image is shown in Figure 4. The image outline is clear and complete in the figure and is basically the same as the outline of the original image.

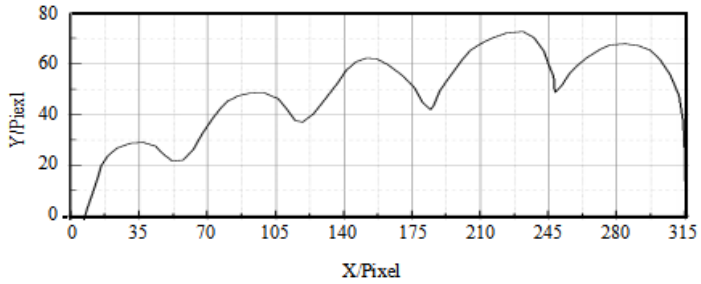

（a）front view of the right mandible

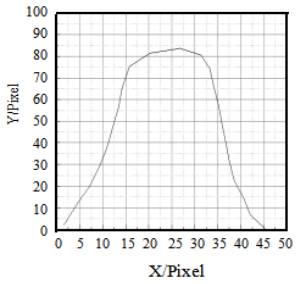

(b) side view of the right mandible

Fig. 4 - Extracted contour line of the ant's mandible teeth

Fitting of the ant maxillary tooth contour curve

The ant maxillary tooth contour curve is relatively complex and difficult to express by a function. To analyse the extracted contour more clearly so that the curve can be expressed accurately, the edge curve of the ant's mandible structure was divided into 5 parts, each corresponding to a peak respectively, as shown in Figure 5.

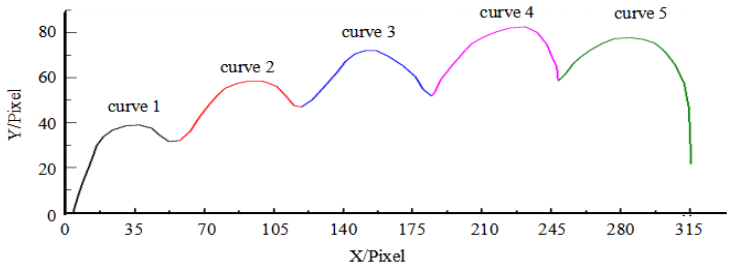

Fig. 5 - Division of extraction curves

Origin software was used for curve fitting, and the least squares method was used to fit each part of the curve. After several attempts, the quintic polynomial function was used to express the contour curve. The function contains 6 parameters, and the fitting equation is expressed as follows:

$$y(x) = Intercept + B_1x + B_2x^2 + B_3x^3 + B_4x^4 + B_5x^5 \quad (3)$$

The fitting results are listed in Table 1:

Curve parameters of the tooth **Table 1**

Parameter	Curve 1	Curve 2	Curve 3	Curve 4	Curve 5
Intercept value	3.18238	918.76187	-134094.10855	342796.87567	-2.27507E6
Intercept standard error	0.13316	183.29073	46153.1945	95347.91022	897390.81551
B_1 value	18.64683	-1066.19397	101804.68471	-216847.35946	1.24004E6
B_1 standard error	0.81429	210.53776	34731.86361	60858.72139	492869.99951
B_2 value	-21.34275	488.22202	-30873.75448	54804.52792	-270226.71585
B_2 standard error	1.56171	95.70713	10445.25828	15529.73055	108232.94174
B3 value	12.13237	-109.45358	4674.85109	-6917.09543	29429.51638
B_3 standard error	1.25171	21.52506	1569.23089	1980.36319	11878.80257
B_4 value	-3.47791	12.03206	-353.40152	435.98646	-1601.79382
B_4 standard error	0.43884	2.39568	117.7696	126.20193	651.58614
B_5 value	0.38642	-0.52015	10.66953	-10.9788	34.85725
B_5 standard error	0.05578	0.10559	3.53224	3.21527	14.29048
Adj.R^2	0.9932	0.9836	0.9955	0.99821	0.98548

A curve fitting variance R^2 closer to 1 indicates a better curve fitting effect and a more realistic fitted function. Table 1 shows that the fitting variances R^2 of all five curves exceed 0.98, indicating a fairly high degree of curve fitting. As observed, the quintic polynomial fitting satisfies the fitting requirements. The side contour curve of the ant's mandible structure was the quintic polynomial function. The result of the fitting is shown in Figure 6, and the fitting equation is expressed as follows:

$$y(x) = 0.13383 + 0.58579x - 0.15297x^2 + 0.29687x^3 - 0.05684x^4 + 0.00282x^5 \quad (4)$$

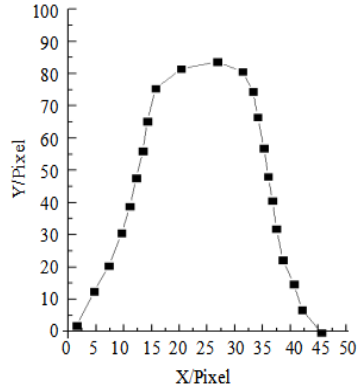

Fig. 6 - Fitted curve of mandible side contour

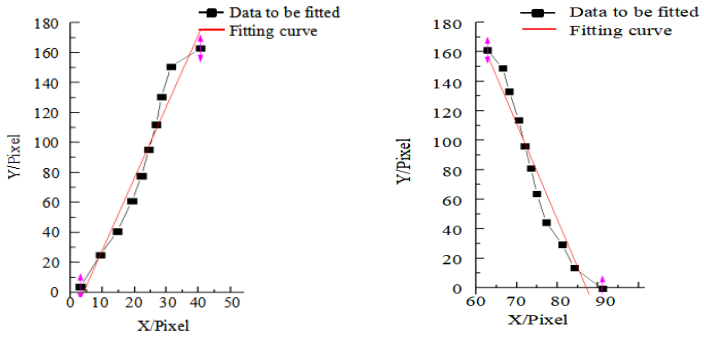

(a) left contour curve (b) right contour curve

Fig. 7 - Fitted line of the mandible side contour

The curve fitting variance R^2 is 0.96513 and it satisfies the fitting requirements. To reduce the machining difficulty of the cutting blade and maintain the bionic character, the least square method was used to fit the left and right contour parts of the curve, as shown in Figure 7. The fitting equation of the left contour curve is expressed as Equation (5), in which the fitting variance R^2 is 0.951563 and the slope is 2.392. The fitting equation of the right contour curve is expressed as Equation (6), in which the fitting variance R^2 is 0.93423, and the slope is -3.23448.

$$y(x) = -2.35631 + 2.392x \quad (5)$$

$$y(x) = 32.42474 - 3.23448x \quad (6)$$

If the accuracy requirements are not high, a straight line can also be used to approximate the upper and lower contour curves of the ventral teeth to simplify the processing technique. The angle between the upper and lower contour lines is 38°.

Analysis of the ant mandible contour curve

The second derivative reflects the slope change rate, and the image of the function is the concave and convex shape of the function (*Zhang et al., 2018*). The second derivative function is obtained for the five fitting polynomial functions, and the graph is plotted for comparative analysis, as shown in Figure 8. Based on Figure 8, the second derivative function of curves 1-5 are generally less than 0. Similar rules apply to curve 1 and curve 2. The second derivative of curve 1 and curve 2 fluctuates between positive and negative values. For curve 3, it begins to decrease at the beginning and increases at the end. Curve 4 and curve 5 have the same rules, it is generally less than 0. The second derivative of the function may reflect the bending direction of the plane curve. When it is greater than, less than, or equal to 0, the image is concave, convex, or neither, respectively. Since the shapes of curve 5 protrude outward, this indicates that the cutting area between the teeth and material is enlarged during cutting, thereby increasing the sliding cutting angle and improving the cutting efficiency, which is conducive to ant feeding. Furthermore, the teeth corresponding to curves 1–5 play a key role in the ant feeding process.

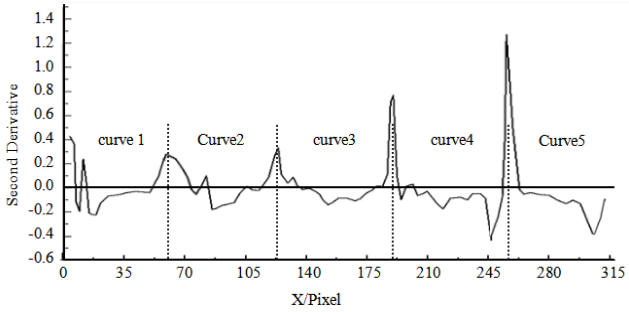

Fig. 8 - Second derivative of the fitted curves with

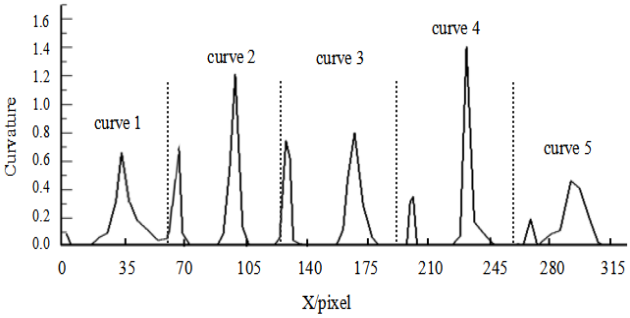

Fig. 9- Curvature of fitted curves with mandible

Curvature is a measure of the degree of non-planarity of the geometry, which can represent the degree of bending of the curve. The greater the curvature, the greater the degree of bending of the curve. The second derivative of the fitted contour curve was calculated, and the curvature of the fitted function was plotted, as shown in Figure 9.

Based on Figure 9, curve 4 has the largest curvature, followed by curves 2 and 3, and curves 1 and 5 have the smallest curvatures. This means that the teeth corresponding to curve 4 are the sharpest and most convex, and therefore the most suitable for cutting. Therefore, in this study, the structural parameters of the fourth tooth of the ant mandible are selected as bionic elements for bionic blade design.

Design and machining of the bionic blade

For comparative analysis, the same structural parameters were used for the bionic blade as in the case of the ordinary flat blade (i.e., *a*=180 mm; *b*= 55 mm; *c*=10 mm; *d*=10 mm; α= 38°). The cutting edge of the bionic blade is represented by the contour curves of the fourth teeth of the ant mandible. Comparing the design of the flat and bionic blades, the difference between the blades is mainly in the cutting edge, as shown in Figure 10. Due to the complex structure of the bionic blade, the blade was made via 3D printing to accurately express the bionic elements (*Chaturvedi et al., 2019*). The BLT-T320 metal 3D printer produced by Xi'an Bright Laser Technologies Co., Ltd. was selected, and the 3D printing material was 316L stainless steel made of fine metal powder.

At a test temperature of 24.8 ℃, the material tap density was measured to be ≥ 4.75 g/cm^3, the tensile strength was 586–649 MPa, the yield strength was 265–382 MPa, and the elastic modulus range was 205–265 GPa. Using direct metal laser sintering technology, the laser beam combines the metal powder layer and fusion point to form the blade. After processing, the bionic blade is clear and complete, with a smooth blade surface. The 3D printed blade is shown in Figure 11.

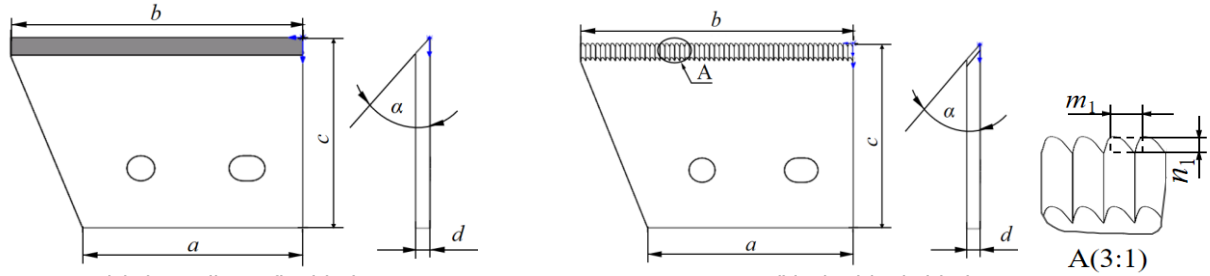

(a) the ordinary flat blade (b) the bionic blade

Fig. 10 - Structural mode of the blades

(a) the ordinary flat blade (b) the bionic blade

Fig. 11 -Samples of the blade

Finite element analysis of the blades

The reliability of the blade directly affects the working efficiency of the device when cutting the stalks. A finite element analysis of the ordinary flat blade and the bionic blade were conducted, and the software used was ANSYS 2020. Defined as the structural steel, the material of the ordinary flat blade and the bionic blade was evaluated; the material properties of the ordinary flat blade and bionic blade were described in Table 2. A finite element analysis was conducted on the blade after being meshed.

Material parameter **Table 2**

Parameters	Value	Units
Structural steel	0.3	-
Elastic Modulus	2.0×10^5	MPa
Density	7.85×10^3	Kg/m^3
Yield Strength	305	MPa

Cutting performance test

The texture analyser is immune to human error, has objectivity, can improve data authenticity, stability, and repeatability, and can be used to measure the material's mechanical properties, such as tissue structure characteristics and cutting resistance. The cutting performance test of the blade was performed with the Shanghai TengBa Rapid TA practical texture analyser, as shown in Figure 12.

Fig. 12 -Test system

When the blade moves down to cut the corn stalks, the configured software system automatically records the cutting resistance and time, cutting resistance and displacement, and time and displacement curves of the blade. In this experiment, the loading speed of 5 mm/s and 10 mm/s were selected for the cutting performance test to analyse the effects of the conventional flat blade and the bionic blade on corn stalk cutting. The test sample is taken from the corn test field of Shenyang Agricultural University. The corn stalk is cut in the same condition and with an average moisture content of 73.8 %.

RESULTS AND ANALYSIS

Analysis of Finite element of blades

As it is shown in Fig. 13, the maximum stress on the ordinary flat blade (33.345 MPa) and the bionic blade (26.526 MPa) are observed at the threaded hole on the right side. Compared with that of the flat blade, the maximum stress of the bionic blade is 20.45% lower. The maximum stress on the ordinary flat blade and the bionic blade are considerably less than 355 MPa. Thus, the strength of the blades meets the requirements of mechanical properties. Furthermore, the total deformation of the ordinary flat blade and bionic blade is 6.1549×10-3 and 4.8942×10-3, respectively. Compared with that of the flat blade, the total deformation of the bionic blade is 20.48% lower. Accordingly, within the safe range, the deformation resistance of the ordinary flat blade and bionic blade are satisfactory, and the bionic blade is more suitable than the ordinary flat blade.

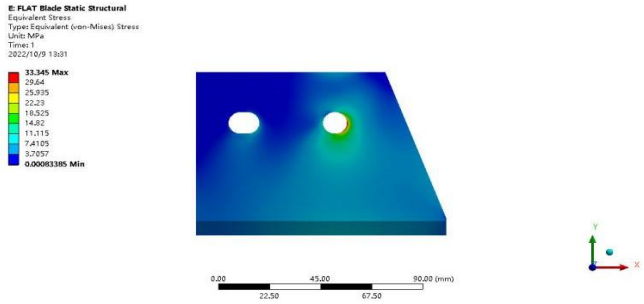

(a) Stress nephogram of the ordinary flat blade

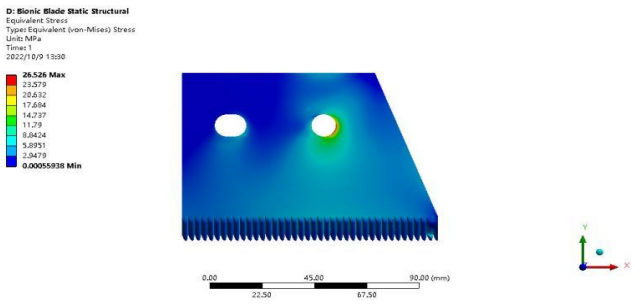

(b) Stress nephogram of the bionic blade

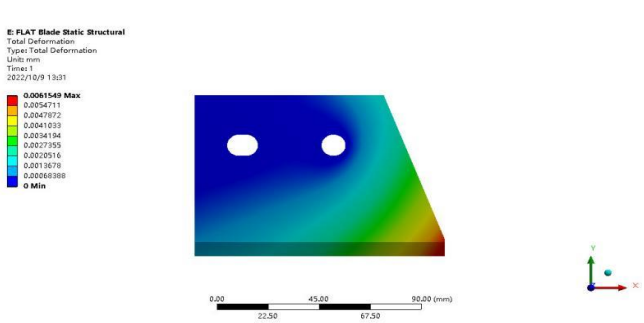

(c) Total deformation nephogram of the ordinary flat blade

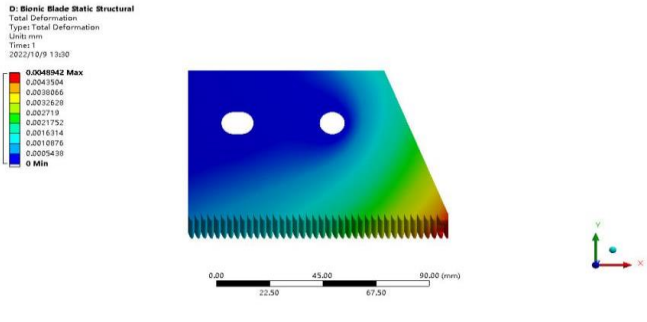

(d) Total deformation nephogram of the bionic blade

Fig. 13 - Results of Finite element analysis of blades

Analysis of the blades on the corn stalk cutting force

Cutting force is a key factor that reflects the cutting efficiency. The relationship between cutting force and displacement is shown in Figure 14.

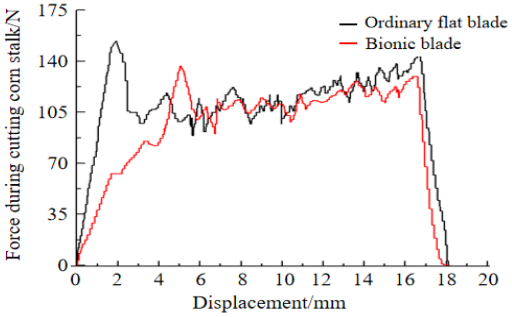

Fig. 14 - Relationship between the cutting force and displacement

When a normal flat blade was used, the cutting force rapidly increased during the displacement from zero to 2 mm. Then, the force decreased and remained in a vibration state that lasted almost until the end of the cutting operation. Toward the end of the cutting process, the forces increased again, reached a maximum, and then promptly dropped to zero. For the bionic blade, the cutting force increased slowly, and the vibration state persisted until the end of cutting. For the bionic blade the cutting force increased from zero to 1 mm and from 4 to 6 mm during the displacement. The maximum forces when cutting corn stalks with the two types of blades are different. The maximum forces in the experiments are listed in Table 3.

Table 3

Maximum force during cutting corn stalk

Loading speed/ mm·s^{-1}	No.	Maximum cutting force/N	
		Ordinary flat blade	Bionic blade
5	1	149.24	131.13
	2	153.52	138.87
	3	167.29	142.83
	4	164.13	140.34
	5	159.11	136.28
	6	150.38	134.22
	7	147.79	133.58
	8	152.57	141.21
	Average	155.50	137.31
10	1	151.83	138.49
	2	158.03	141.35
	3	170.57	151.54
	4	167.62	152.78
	5	165.25	140.17
	6	155.74	142.03
	7	156.81	137.08
	8	158.33	147.62
	Average	160.52	143.88

Under a loading speed of 5 mm/s, the maximum cutting forces of the flat blade and bionic cutter were 155.50 N and 137.31 N, respectively. Compared with that of the flat blade, the maximum cutting force of the bionic blade was 11.70% lower. Under a loading speed of 10 mm/s, the maximum cutting forces of the flat blade and bionic cutter were 160.52 N and 143.88 N, respectively. Compared with that of the flat blade, the maximum cutting force of the bionic blade was 10.37% lower.

The average cutting force when cutting the corn stalk using the ordinary and bionic blades are shown in Figure 15. Under a loading speed of 5 mm/s, the average cutting forces of the ordinary flat and bionic blades were 109.21 N and 96.56 N, respectively. Compared with that of the ordinary flat blade, the average cutting force of the bionic blade was 11.58 % lower. Under a loading speed of 10 mm/s, the average cutting forces of the ordinary flat and bionic blades were 111.97 N and 101.03 N, respectively. Compared with that of the ordinary flat blade, the average cutting force of the bionic blade was 9.77 % lower. This indicates that the bionic blade can reduce the cutting force. There is a statistically significant difference between the data of the four groups at the 0.05 level, indicated by the letters a, b, c and d. The standard deviation of the average cutting force of the ordinary flat blade is larger than that of the bionic blade, indicating that the average force of the bionic blade is similar.

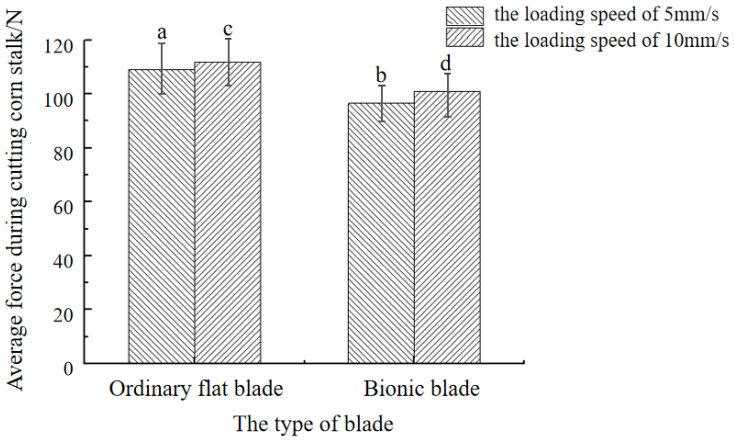

Fig. 15 - Average cutting force

When cutting the straw husk, the required cutting force is 63–83 %, and the cutting force was greater at the beginning and end of cutting. The maximum cutting force of the cutting process was often instantaneous. The greater the instantaneous cutting force, the easier it is to damage the blade during cutting. The maximum transient cutting force of the bionic blade was lower than that of the ordinary flat blade. This means that the cutting of the bionic blade is gentler than that of the ordinary flat blade. The bionic blade can effectively reduce the instantaneous maximum cutting force, which is closely related to the shape of the bionic blade. The evenly distributed tooth edges increase the sliding cutting angle of the bionic blade and improve the cutting performance.

Analysis of energy consumption during cutting

Energy consumption during cutting is an important factor that reflects the cutting quality. The force–displacement curve can be plotted when the blade cuts the corn stalk at a constant speed. The energy consumption during cutting can be calculated from the area between the cutting force curve and the displacement axis. The average energy consumption of the different types of blades during cutting is shown in Table 4. The average energy consumption for cutting a single corn stalk is shown in Figure 16.

Table 4

Energy consumption during cutting corn stalk

Loading speed/ mm·s^{-1}	No.	Energy consumption /J	
		Ordinary flat blade	Bionic blade
5	1	10.28	9.37
	2	10.76	9.72
	3	11.88	10.12
	4	11.35	9.82
	5	11.03	9.56
	6	10.58	9.55
	7	10.35	9.35
	8	10.95	9.88
	Average	10.90	9.67

Loading speed/ mm·s^{-1}	No.	Energy consumption /J	
		Ordinary flat blade	Bionic blade
10	1	10.50	9.90
	2	11.10	9.89
	3	12.11	10.74
	4	11.59	10.69
	5	11.46	9.831
	6	10.96	10.11
	7	10.98	9.60
	8	11.36	10.33
	Average	11.26	10.14

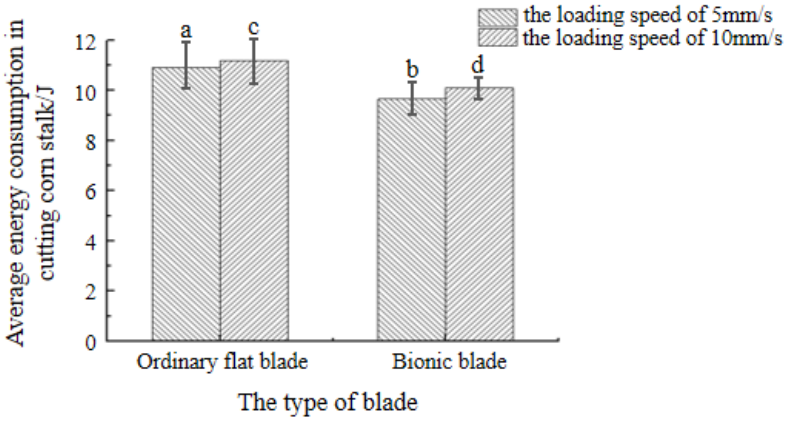

Fig. 16 - Average energy consumption during cutting

Under a loading speed of 5 mm/s, the average power consumption of the flat and bionic blades was 10.90 and 9.67 J, respectively. Compared with the flat blade, the average power consumption of the bionic blade was 11.28% lower. Under a loading speed of 10 mm/s, the average power consumption of the flat and bionic blades was 11.26 and 10.14 J, respectively. Compared with the flat blade, the average power consumption of the bionic blade was 9.95% lower. Due to the different blade types, the average energy consumption during cutting were significantly different. The bionic blade consumed less energy than the flat blade. Therefore, the bionic blade is more suitable for cutting stalks than the flat blade.

CONCLUSIONS

(1) Inspired by the unique geometric structure of ant mandibular teeth, based on the microscopic photography technology and image processing technology to obtain information about the profile curve of the ant mandibular teeth, up to the palate of the profile tooth curve fitting, our analysis concluded that the fourth tooth of the ant mandibular is the most prominent and sharpest, and can be used as a bionic prototype to design and manufacture a new type of bionic blade. Moreover, to carry out finite element static analysis of blades, ANSYS software was applied. The results corroborated the strength and stiffness of the designed bionic blade were better than those of the ordinary flat blade.

(2) To compare the cutting performance of the bionic and the ordinary flat blade, the bionic and ordinary flat blade were manufactured using metal 3D printing technology. The cutting performance of the bionic blade and the ordinary flat blade was tested using the Rapid TA practical texture instrument. Under a loading speed of 5 mm/s, the maximum cutting force of the bionic blade is 11.70 % lower than that of the ordinary flat blade, and the average cutting force of the bionic blade is 11.58 % lower than that of the ordinary flat blade. The average energy consumption of the bionic blade is 11.28 % lower than that of the plain blade during cutting. Under a loading speed of 10 mm/s, the maximum cutting force of the bionic blade is 10.37 % lower than that of the ordinary flat blade, and the average cutting force of the bionic blade is 9.77 % lower than that of the ordinary flat blade. The average energy consumption of the bionic blade is 9.95 % lower than that of the plain blade during cutting. The results show that the bionic blade can effectively reduce the cutting force and energy consumption and is more suitable for cutting corn straw.

(3) In this study, the cutting force and power consumption of the two blades were tested only at quasi-static velocity. Therefore, the cutting performance of the bionic blade at dynamic speed should be further investigated in future research.

ACKNOWLEDGEMENT

This research was funded by the scientific effort of Liaoning Agricultural Technical College (Lnz202216).

REFERENCES

[1] Chaturvedi A, Bhatkar S, Sarkar PS, et al., (2019), 3D geometric modelling of aluminium based foam using micro computed tomography technique, *Materials Today: Proceedings*, Vol.18, Issue 7, pp. 4151-4156, Mumbai / India;

[2] Chen Pan, Xu Pengfei, (2021), Simulation analysis and mechanism study on drag reduction of “Bionics” groove（"仿生学"沟槽减阻仿真分析及机理研究）. *Aeroengine*, Vol.47, Issue 2, pp. 28-32, Shen Yang / P.R.C;

[3] Jia Honglei, Li Changing, Zhang Zhihong et al., (2013), Design of bionic saw blade for corn stalk cutting. *Journal of Bionic Engineering*, Vol.10, Issue 4, pp.497-505, Ji Lin / P.R.C;

[4] Jia Honglei, Tan Hewen, Ma Zhongyang et al., (2022), Design and experiment of the straw breaking and diversion device for maize harvesters (玉米收获机断秸导流装置设计与试验). *Transactions of the Chinese Society of Agricultural Engineering,* Vol.38, Issue 4, pp.12-23, Ji Lin / P.R.C;

[5] Lei Yanyuan; Lv Lihua; Shi Qingxing, et al., (2016), Morphological and ultrastructural observation of mandibles of two invasive fire ants（两种火蚁与黑头酸臭蚁上颚形态及其超微结构观察）, *Journal of Environmental Entomology*, Vol.38, Issue 6, pp.1199-1204, Guangzhou / P.R.C;

[6] Ma Pengbo, Li Liqiao, Wen Banqin et al., (2020), Design and parameter optimization of spiral-dragon type straw chopping Test Rig. *Int J Agric & Biol Eng*, Vol.13, Issue 1, pp.47-56, Shi Hezi/ P.R.C;

[7] Massah Jafar, Hassanpour Fatemeh, Roudbeneh Zeinab Hassanpour et al., (2020), Experimental investigation of bionic soil-engaging blades for soil adhesion reduction by simulating Armadillidium vulgare body surface. *INMATEH-Agricultural Engineering*, Vol.60, Issue 1, pp. 99-106, Bucharest / Romania.

[8] Paul J., Roces F. et al., (2003), Fluid intake rates in ants correlate with their feeding habits, *Journal of Insect Physiology*, Vol.49, Issue 4, pp.347-357, Würzburg / Germany;

[9] Tian Kunpeng, Li Xiangwang, Shen Chen, et al., (2017), Design and test of cutting blade of cannabis harvester based on longicorn bionic principle (天牛仿生大麻收割机切割刀片设计与验), *Transactions of the Chinese Society of Agricultural Engineering,* Vol.33, Issue5, pp. 56－61, Nan Jing / P.R.C;

[10] Tong Jin, Xu Shun et al., (2017), Design of a bionic blade for vegetable chopper, *Journal of Bionic Engineering*, Vol.14, Issue 1, pp.163-171, Ji Lin / P.R.C;

[11] Xu Kai, Ge Yanyan, Xiao Maohua et al., (2021), Design of a straw picking and cutting device. *Int J Agric & Biol Eng*, Vol.14, Issue 6, pp.93–98, Shan Dong / P.R.C;

[12] Zhang Anlun, Teng Guowei, Zhao Haiwu et al., (2018), Video background modelling algorithm with low complexity based on the minimum second derivative (基于最小二阶导数的低复杂度视频背景建模算法), *Journal of Optoelectronics Laser,* Vol.29, Issue 8, pp. 858-864, Shanghai / P.R.C;

[13] Zhang Chenyang, Ding Bing, He Zhongqiang et al., (2022), Kinematics analysis and optimization of rotary multi-legged bionic robot (转盘式多足仿生机器人的运动学分析及优化). *Chinese Journal of Engineering Design*, Vol.29, Issue 3, pp.327-338, Shang Hai / P.R.C;

[14] Zhang Xuening, You Yong, Wang Decheng et al., (2022), Design and experiment of a combined root-cutting and ditching device, *INMATEH-Agricultural Engineering*, Vol.66, Issue 1, pp.383-392, Bucharest / Romania.

[15] Zhao Jiale, Guo Mingzhuo, Lu Yun et al., (2020), Design of bionic locust mouthparts stubble cutting device. *Int JAgric & Biol Eng*, Vol.13, Issue 1, pp. 20-28, Ji Lin / P.R.C;

[16] Zhao Zhu, Wang Zhongnan, Zhao Bintong et al., (2022), Designing a longitudinal hob-type stalk chopping device for corn combine harvester, *INMATEH-Agricultural Engineering*, Vol.67, Issue 2, pp.41-52, Bucharest / Romania.